

# Synthesis and Characterization of the Zinc Ferrite (ZnFe<sub>2</sub>O<sub>4</sub>) Nano Powder for Anticancer Activity

K. Tharani<sup>a</sup>, L.C. Nehru<sup>a\*</sup>, M.Muthuselvam<sup>b</sup>, S.Arumugam<sup>c</sup>

<sup>a</sup>Department of Medical Physics, Bharathidasan University, Tiruchirappalli, Tamilnadu

<sup>b</sup>Department of Biotechnology, Bharathidasan University, Tiruchirappalli, Tamilnadu

<sup>c</sup>Department of Physics, Bharathidasan University, Tiruchirappalli, Tamilnadu, India

## Abstract

ZnFe<sub>2</sub>O<sub>4</sub> nanopowder was prepared by the solution combustion method. In this method, urea as organic fuel agent. The structure of the prepared nanopowder was characterized by powder X-ray Diffraction (PXRD), Fourier transform infrared (FT-IR), Vibrating sample magnetometer (VSM) and UV-visible spectroscopy. The XRD result conforms the formation of spinel cubic structure with Fd $\bar{3}$ M space group matches with ICDD No.82-1042. The average particle size calculated by Debye Scherer formula is 33 nm. The shape and morphology were studied by Field Emission Scanning Electron Microscope (FESEM) and confirms the nanopowder size which falls in the range from 20 to 25 nm. In this study, antibacterial and in vitro anticancer properties of zinc ferrite nano powder were evaluated. Antibacterial activity of zinc ferrite was studied against E.coli pathogenic bacteria and In vitro anticancer activity was screened by cell viability assay test. The result shows that the zinc ferrite nano powder have been used for antimicrobial and anticancer activity. It reveals that the zinc ferrite nano particles have medical applications.

**Keywords:** ZnFe<sub>2</sub>O<sub>4</sub>, Antimicrobial and Anticancer activity.

## Introduction:

The most promising feature of nanotechnology is the magnetic nano particles (MNPs) of different compositions<sup>1</sup>. They offer remarkable applications in the fundamental and technological field such as biomedical, bio processing and catalysts among many others<sup>2-5</sup>. Zinc belongs to a class of microelements that is considered to play an important role in many vital biochemical reactions and physiological processes: growth and development of the cells, stimulation of the gene transcription and cell proliferation, slowing down the oxidation processes, optimization of the human immune system<sup>6-8</sup>. Therefore, to get more information about zinc ferrite nano particles (ZnO·Fe<sub>2</sub>O<sub>3</sub>) and to improve their applications or develop new ones, careful studies related to their functionality, particle sizes and also their antimicrobial behavior are essential. Among the spinel ferrite compounds Zinc Ferrite (ZnFe<sub>2</sub>O<sub>4</sub>) exhibits super paramagnetic behavior and it has potential application in many fields, such as photocatalysis, magnetic resonance imaging (MRI), Li-ion batteries and gas sensors. Various synthesis methods are proposed to prepare ZnFe<sub>2</sub>O<sub>4</sub> nano particles such as co-precipitation, combustion, thermal decomposition, solvothermal, hydrothermal, ball milling, and ceramic route techniques. Among the synthesis methods the hydrothermal method has been widely used, because of its simplicity, low cost, nontoxic route and yields crystalline nano materials in a short time. In this work super paramagnetic ZnFe<sub>2</sub>O<sub>4</sub> nano particles were synthesized by hydrothermal method using the capping agents<sup>9-15</sup>.

In this work, zinc-doped magnetite nano particles are synthesized through by combustion method using PEG as capping agent. To characterize structure and morphology of nanoparticles by Powder X-ray Diffraction (P-XRD), Fourier Transform Infrared (FT-IR)

and UV-visible spectroscopy. To evaluate the properties of synthesized nano particles by quenching study, anti-bacterial and *invitro* anticancer activity. This method may be the mostpromising one because of its simplicity and productivity. It is widely used for biomedical applications because of the ease of implementation and the need for less hazardous materials and procedures.

## MATERIALS AND METHODS

### Synthesis and characterization

ZnFe<sub>2</sub>O<sub>4</sub> Nano particles were prepared by solution combustion method. Stoichiometric amounts of Ferric nitrate Fe(NO<sub>3</sub>)<sub>3</sub>.9H<sub>2</sub>O and Zinc nitrate Zn(NO<sub>3</sub>)<sub>2</sub>.6H<sub>2</sub>O and Urea were dissolved in deionized water and poured into a quartz container can be mixed well by magnetic stirrer for 30 minutes, which make them almost as homogeneous mixtures, which was placed in a muffle furnace heated at 300°C. Initially, the solution boils and undergoes dehydration followed by decomposition with the evolution of large amount of gases with white fumes coming out from the exhaust opening provided on the top of the furnace. After the solution reaches the point of spontaneous combustion, it begins burning and releases lots of heat, vaporizes all the solution instantly and becomes a foamy white solid powder. Urea serves as fuel, being oxidized by nitrate.

The synthesized ZnO& ZnFe<sub>2</sub>O<sub>4</sub> powder was characterized by powder X-ray diffraction (Bruker Advanced D8) with Cu-K $\alpha$  radiation. Ultraviolet visible-near infrared (UV-Vis) studies were carried out in the range of 300–450 nm using Perkin Elmer UV-Vis (Model-lambda35) Spectrophotometer. The surface morphology of the sample was analyzed using a Scanning Electron Microscope (SEM) (Hitachi 3000 H). The magnetic properties of the investigated solids were measured at room temperature using a Vibrating Sample Magnetometer (VSM; 9600-1 LDJ). The test organisms, Escherichia coli (MTCC2412) and Staphylococcus aureus (MTCC2412) bought from Microbial Type Culture Collection IMTEC, India.

### Animal Cell Culture:

The A549 human lung cancer cell line was obtained from National Center for Cell Science (NCCS), Pune, India. The cells were cultured in DMEM high glucose medium (Sigma-Aldrich, USA), supplemented with 10% fetal bovine serum (Gibco), and 20 mL of penicillin/streptomycin as antibiotics (Gibco), in 96 well culture plates, at 37 °C in a humidified atmosphere of 5% CO<sub>2</sub> in a CO<sub>2</sub> incubator (Thermo scientific, USA). All experiments were performed using cells from passage 15 or less.

### Cell Viability Assay:

The cell viability was measured using a standard MTT-assay. The complex, ZnO and ZnFe<sub>2</sub>O<sub>4</sub> was first dissolved in dimethyl sulfoxide (DMSO) to make a stock. These stock solutions were diluted separately with media to get various concentrations of the complex. Two hundred micro liters of these samples were added to wells containing 5 X 10<sup>3</sup> A549 cells per well. DMSO solution was used as the solvent control. After 24 h, 20  $\mu$ l of MTT solution (5mg/mL in PBS) was added to each well and the plate was wrapped with aluminum foil and incubated for 4 h at 37 °C. The purple formazan product was dissolved by addition of 100  $\mu$ L of DMSO to each well. The absorbance was monitored at 570 nm (measurement) and 630 nm (reference) using a 96-well plate reader (Bio-Rad, iMark, USA). Data were collected for three replicates each and used to calculate the respective mean. The percentage inhibition was calculated, from this data, using the formula:

$$\frac{\text{Mean absorbance of untreated cells (Control)} - \text{Mean absorbance of treated cells}}{\text{Mean absorbance of untreated cells (Control)}} \times 100$$

### Acridine orange (AO) and ethidium bromide (EB) staining

Apoptotic morphology was investigated by AO/EB double staining method as described by Spector et al with some modifications. Briefly, the cells treated with  $IC_{50}$  Concentration of compounds for 24 h. After incubation, the cells were harvested and washed with cold PBS. Cell pellets were resuspended and diluted with PBS to a concentration of  $5 \times 10^5$  cells/mL and mixed with 25  $\mu$ L of AO/EB solution (3.8  $\mu$ M of AO and 2.5  $\mu$ M of EB in PBS) on clean microscope slide and immediately examined under fluorescent microscope (Carl Zeiss, Axioscope2plus) with UV filter (450–490 nm). Three hundred cells for each sample were scored for viable, apoptotic or necrotic by staining the nucleus structure and membrane integrity and the percentage of apoptotic and necrotic cells were calculated accordingly.

### Result & discussion:

#### XRD Spectrum of ZnO and ZnFe<sub>2</sub>O<sub>4</sub> nanopowder:

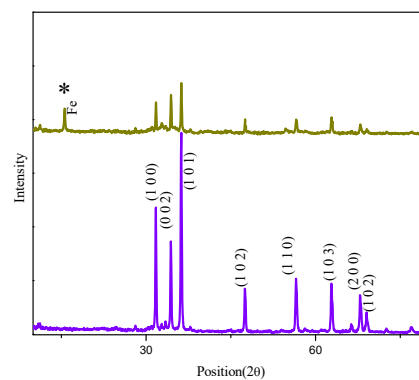


Fig (1) Shows XRD Spectrum of ZnO and ZnFe<sub>2</sub>O<sub>4</sub>

An X-ray diffraction (XRD) pattern of the ZnO&ZnFe<sub>2</sub>O<sub>4</sub> nanopowder is as shown in fig (1). It will match with the ICDD No. 82-1042. The XRD pattern showing that  $2\theta=31^\circ, 34^\circ, 36^\circ, 47^\circ, 56^\circ, 63^\circ, 67^\circ$ . The peaks found in angle are labeled as (1 0 0), (0 0 2), (1 0 1), (1 0 2), (1 1 0), (1 0 3), (2 0 0) and the lattice constant was calculated using d- value and with their respective (h k l) parameters. The average particle size is 33 nm. The ZnO nanoparticles have a hexagonal wurtzite structure. From ZnFe<sub>2</sub>O<sub>4</sub> no secondary phase of any Fe(III) oxide was detected.

#### FTIR Spectrum of ZnO and ZnFe<sub>2</sub>O<sub>4</sub> nanopowder:

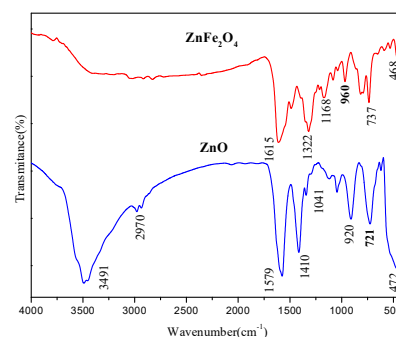
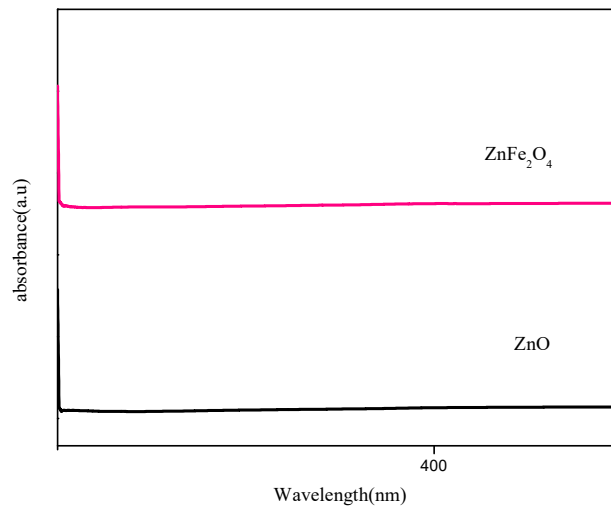


Fig (2) FTIR Spectrum of ZnO & ZnFe<sub>2</sub>O<sub>4</sub>

Fig (2) exhibits the typical FT-IR spectrum of ZnO in the scale range between 4000-400 $\text{cm}^{-1}$ . The finger print of ZnO occurs mainly at 472 $\text{cm}^{-1}$ , where a strong sharp peak corresponds to Zn-O-Zn stretch of metallic group is present in the sample. The peak 720  $\text{cm}^{-1}$  aromatic C-H bending is present. The peak 920  $\text{cm}^{-1}$  OH group is present. The peak 1041  $\text{cm}^{-1}$  represents O-H group. The peaks 1410 & 1579  $\text{cm}^{-1}$  C-O stretching are present. The peaks 2970  $\text{cm}^{-1}$  represent to the alkane (C-H) stretching. Amines (doublet for NH<sub>2</sub>) stretching is present in the peak of 3491. In graph (2b) exhibits the typical Fourier Transform Infrared (FTIR) spectrum of ZnFe<sub>2</sub>O<sub>4</sub> nanoparticles at room temperature. The synthesized ZnFe<sub>2</sub>O<sub>4</sub> exhibits various well-defined peaks at 468, 737, 960, 1168, 1322 and 1615 $\text{cm}^{-1}$ . Generally 1000 $\text{cm}^{-1}$  metal group is present. The peak 1168  $\text{cm}^{-1}$  is assigned to C-O stretching. The peak 1322  $\text{cm}^{-1}$  is denoted to NO<sub>2</sub> stretching.

#### UV Spectrum of ZnO and ZnFe<sub>2</sub>O<sub>4</sub> nanopowder:

Fig(3) shows the UV- Vis absorption Spectra of Zinc Oxide nanoparticle as a function of wavelength in the wavelength range between 200-1000nm. The excitation wavelength was presented in 207nm. The band gap energy of the ZnO nanoparticle is 5.7eV.



Fig(3) UV-Vis Spectrum of ZnO & ZnFe<sub>2</sub>O<sub>4</sub>

#### SEM SPECTRUM:

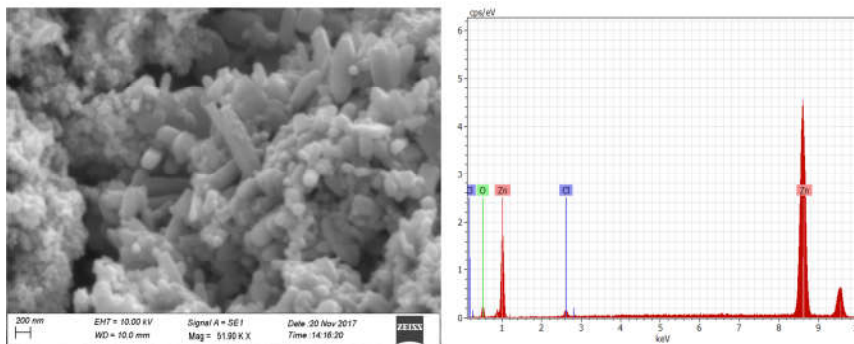


Fig 4(i) SEM with EDX Spectrum of ZnO



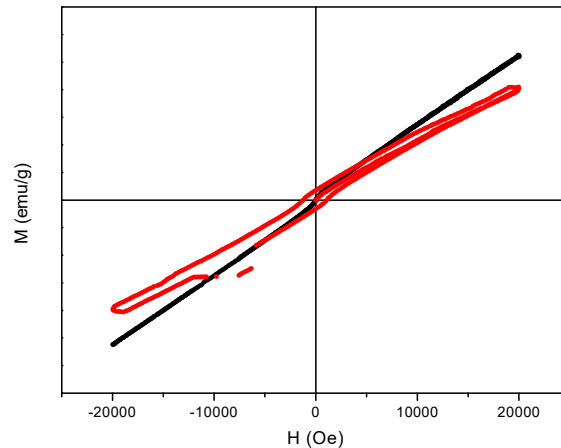


Fig (6) Shows VSM Spectrum of ZnO& ZnFe<sub>2</sub>O<sub>4</sub>

#### Antibacterial activity:

Fig (7) shows antibacterial activity of both gram positive (*Staphylococcus aureus*), gram negative (*Escherichia coli*) of ZnO& ZnFe<sub>2</sub>O<sub>4</sub>. Here 10( $\mu$ g/ $\mu$ l) concentration of ZnO&ZnFe<sub>2</sub>O<sub>4</sub> taken. From fig ZnO is denoted A&ZnFe<sub>2</sub>O<sub>4</sub> is denoted C. The diameter of zone of inhibition of ZnO - gram positive is 2.9cm,gram negative 2.7cm. Similarly ZnFe<sub>2</sub>O<sub>4</sub> - gram positive is 3.1cm,gram negative 2.7cm.

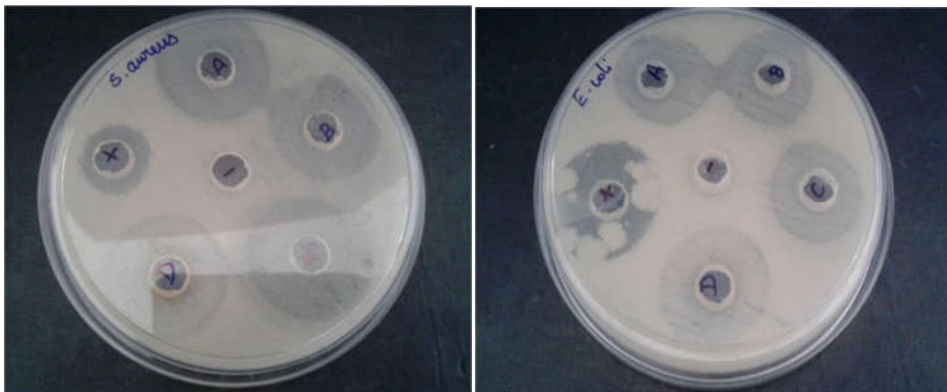


Fig7 Anti-bacterial activity of (i) gram-positive, (ii) gram- negative bacteria

#### Cell Viability Assay:

The cytotoxic activities of all the complexes have been investigated against the A549 human lung cancer cell line by using MTT assay (Mosmann T, 1983). The cytotoxic activity was determined according to the dose values of the exposure of the complex required to reduce survival to 50% (IC<sub>50</sub>), compared to untreated cells. The observed IC<sub>50</sub> values for 24 h reveal that all the complexes exhibit different range of cytotoxicity (Figure 8). The ability of the complexes to kill the cancer cells at 24 hour incubation vary as ZnO> ZnFe<sub>2</sub>O<sub>4</sub>. The results from this MTT assay indicate that the ZnO and ZnFe<sub>2</sub>O<sub>4</sub> samples are toxic to the A549 cells.

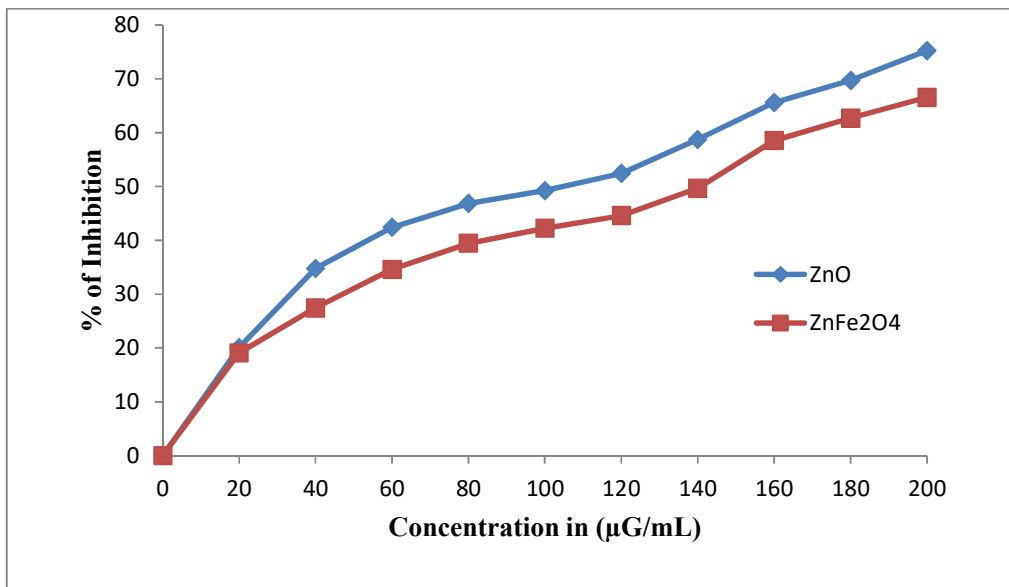


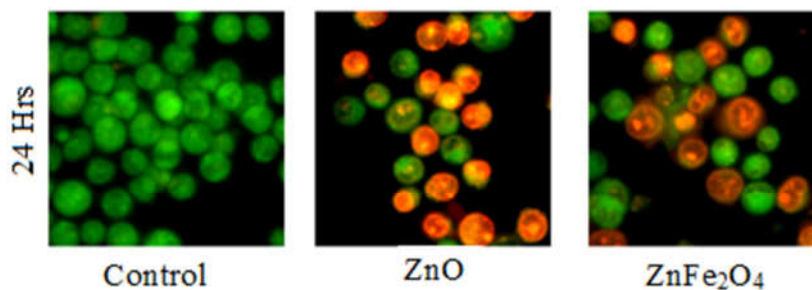
Figure (8): Anti-proliferative effect of complexes against the A549 cells

Compound	IC <sub>50</sub> Values (24 h) (µG/mL)
ZnO	110 ± 0.05
ZnFe <sub>2</sub> O <sub>4</sub>	140 ± 0.05

Table 1. In vitro cytotoxicity assays for the complex against human lung cancer cell line (A549)

**Acridine orange (AO) and ethidium bromide (EB) staining:**

The most important characteristics of apoptosis are morphological changes during cell death. Figure 1 represents that AO/EB double-stained A549 human lung cancer cell line treated with test substances 24 hr underwent both early apoptosis (cells with red arrows) and late apoptosis. The control or viable cells shows green fluorescence and normal cell features of uniform chromatin with an intact cell membrane, whereas, the early apoptosis cells showed bright green region with yellowish green nuclear fragmentation and membrane bubbles and apoptotic bodies outside. The late apoptosis cells exhibited orange-yellow or red nuclei with condensed or fragmented chromatin. The results demonstrate that all substances induce majority of cell death through apoptosis mode and very fewer in necrosis for 24 hr treatment. Chromatin condensation and fragmentation were majorly observed in ZnO and ZnFe<sub>2</sub>O<sub>4</sub> treated cells.



Figure(9)Ao/Eb: Control, ZnO,ZnFeO<sub>3</sub> whereas Fe<sub>2</sub>O<sub>3</sub> treated cells. Green colour cells are live cells and Red colour cells showing apoptotic morphology

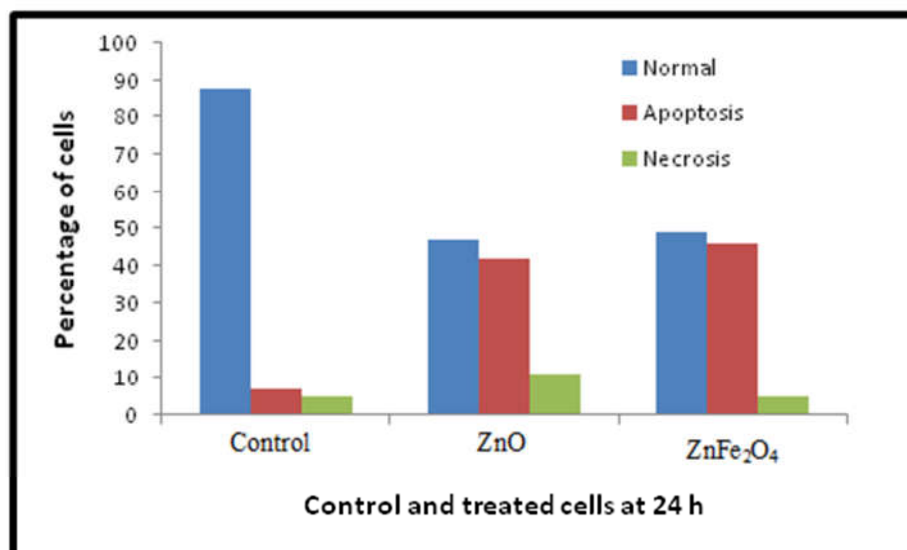


**Fig (10) AO/EB staining to detect the mode of cell death induced by the complexes. Both complexes induces apoptosis mode of cell death majorly. Graph shown manual count of apoptotic cells in percentage.**

#### **Conclusion:**

1. Synthesis of metal oxides such as ZnO and ZnFe<sub>2</sub>O<sub>4</sub> by simple combustion method.
2. The crystalline structure of the prepared metal oxide nanopowders was analyzed by powder X-ray diffraction (XRD). It is very important nondestructive technique very useful characterizing nanoparticles. It address all issues related to nanomaterials, crystal structure, crystallite size, identification of unknown materials, crystals structure, preferred orientation, defects and stresses.
3. Surface characterization techniques provide the possibilities to study individual nanostructures. The fundamental understanding of the relationship between physical thermal properties and materials dimensions needs ultra high resolution imaging techniques. Scanning Electron Microscopy provides the surface morphology of the micro structures of nanostructured materials along with chemical composition and distribution. EDX was used to quantitative composition analysis of the nanomaterials.
4. Analysis of optical absorbance and reflectance spectra of the nanomaterial was measured using a double beam UV-Vis-NIR Spectrometer.
5. Antibacterial activity against Gram-negative and positive bacteria.
6. Anticancer activity against lung cancer (A549) cell line.

#### **Acknowledgements:**

Financially support of this work from DST-PURSE and the author would also thank Mahatmagandhi Doerenkamp Centre, Bharathidasan University, Tiruchirappalli, Tamilnadu, India.

#### **References:**

1. K. Sobha, K. Surendranath and V. Meena, Biotechnology and Molecular Biology Reviews, 5,01 (2010).
2. H. Amekura, O.A. Plaksin, N. Umeda, Y. Takeda, N. Kishimoto and Ch. Buchal., Mater.Res.Soc.Symp.Proc.,1, 8.1.1 (2006).
3. Ho Chan and Ming-Hsun Tsai, Rev.Adv.Mater. Sci.,18,734 (2008).
4. U. Abhulimen, Mater.Res.Soc.Symp.Proc.,1, 27.1 (2005).
5. M. A. Shah and M. Al-Shahry, JKAU: Sci,2,61 (2009).

6. Atul Gupta, H.S.Bhatti, D.Kumar, N.K.Vermaa, R.P.Tandonb. , Journal of Nanomaterials and Biostructures,4,1 (2006).
7. Cheng-Hsien Hsieh, Journal of the Chinese Chemical Society,54,31 (2007)
8. AbdolmajidBayandoriMoghaddam,TayebeNazari, JalilBadragh and Mahmood Kazemzad, Int. J. Electrochem. Sci., 4, 247 (2009).
9. C.P.Rezende, J.B.da Silva, N.D.S. Mohallem, Brazilian Journal of Physics,1,248 (2009).
10. Robert.F.Mulligan, Agis.A.Iliadis and Peter Kofinas, Journal of Applied Polymer Science, 1,1058 (2003).
11. NagarajanPadmavathy,RajagopalanVijayaraghavan,Enhanced Science and Technology of Advanced Material,8, 1 (2008).
12. Investigation of anticancer and antibacterial activities of zinc oxide nanoparticles EmimaJeronsia et al, International Journal of Development Research, 5(10) (2015) 5707.
13. Synthesis, Characterization, and Study of In Vitro Cytotoxicity of ZnO-Fe<sub>3</sub>O<sub>4</sub> Magnetic Composite Nanoparticles in Human Breast Cancer Cell Line (MDA-MB-231) and Mouse Fibroblast (NIH 3T3)GunjanBisht et al, Nanoscale Research Letters 11 (2016) 537.
14. Liu, W.T. Nanoparticles and their biological and environmental applications. J. Biosci. Bioeng. 2006, 102, 1–7.
15. Gulson, B.; McCall, M.J.; Bowman, D.M.; Pinheiro, T. A review of critical factors for assessing the dermal absorption of metal oxide nanoparticles from sunscreens applied to humans, and a research strategy to address current deficiencies. Arch. Toxicol. 2015, 89, 1909–1930.